Tree Physiology 00, 1–14
doi:10.1093/treephys/tpz103

Research paper

Incorporating non-stomatal limitation improves the performance of leaf and canopy models at high vapour pressure deficit

J. Yang[1,7], R. A. Duursma[1], M. G. De Kauwe[2,3], D. Kumarathunge[1], M. Jiang[1], K. Mahmud[1], T. E. Gimeno[4,5], K. Y. Crous[1], D. S. Ellsworth[1], J. Peters[1], B. Choat[1], D. Eamus[6] and B. E. Medlyn[1]

[1]Hawkesbury Institute for the Environment, Western Sydney University, Penrith, NSW 2750, Australia; [2]ARC Centre of Excellence for Climate Extremes, Sydney, NSW 2052, Australia; [3]Climate Change Research Centre, University of New South Wales, Sydney, NSW 2052, Australia; [4]Basque Centre for Climate Change, Scientific Campus of the University of the Basque Country, Leioa 4894, Spain; [5]IKERBASQUE, Basque Foundation for Science, 48008 Bilbao, Spain; [6]School of Life Sciences, University of Technology Sydney, Sydney, NSW 2007, Australia; [7]Corresponding author (jinyan.yang@westernsydney.edu.au)

Received May 8, 2019; accepted September 12, 2019; handling Editor David Whitehead

Vapour pressure deficit (*D*) is projected to increase in the future as temperature rises. In response to increased *D*, stomatal conductance (g_s) and photosynthesis (*A*) are reduced, which may result in significant reductions in terrestrial carbon, water and energy fluxes. It is thus important for gas exchange models to capture the observed responses of g_s and *A* with increasing *D*. We tested a series of coupled *A*–g_s models against leaf gas exchange measurements from the Cumberland Plain Woodland (Australia), where *D* regularly exceeds 2 kPa and can reach 8 kPa in summer. Two commonly used *A*–g_s models were not able to capture the observed decrease in *A* and g_s with increasing *D* at the leaf scale. To explain this decrease in *A* and g_s, two alternative hypotheses were tested: hydraulic limitation (i.e., plants reduce g_s and/or *A* due to insufficient water supply) and non-stomatal limitation (i.e., downregulation of photosynthetic capacity). We found that the model that incorporated a non-stomatal limitation captured the observations with high fidelity and required the fewest number of parameters. Whilst the model incorporating hydraulic limitation captured the observed *A* and g_s, it did so via a physical mechanism that is incorrect. We then incorporated a non-stomatal limitation into the stand model, MAESPA, to examine its impact on canopy transpiration and gross primary production. Accounting for a non-stomatal limitation reduced the predicted transpiration by ~19%, improving the correspondence with sap flow measurements, and gross primary production by ~14%. Given the projected global increases in *D* associated with future warming, these findings suggest that models may need to incorporate non-stomatal limitation to accurately simulate *A* and g_s in the future with high *D*. Further data on non-stomatal limitation at high *D* should be a priority, in order to determine the generality of our results and develop a widely applicable model.

Keywords: hydraulic limitation, model-data assimilation, photosynthesis, stomatal conductance.

Introduction

Vapour pressure deficit (*D*) is the difference between the amount of water vapour that the air can hold at saturation (e_s) and the actual amount of water vapour in the air (e_a; Monteith and Unsworth 2013). With rising air temperature, e_s increases exponentially and as a result *D* is projected to increase strongly in the future (Ficklin and Novick 2017). At the leaf level, as *D* increases and plant water supply becomes limiting, a direct reduction in stomatal conductance (g_s) occurs to limit transpiration, which inevitably also affects photosynthesis (*A*; Cowan and Farquhar 1977). The reduction of *A* and potentially transpiration due to increasing *D* has important implications for global carbon-climate predictions (Reichstein et al. 2013, Will et al. 2013). Thus, it is crucial to understand the response of vegetation to the projected increase in *D* (Novick et al. 2016).

The challenges involved in modelling g_s responses to high D have been discussed since the late 1970s (Cowan 1978; Farquhar 1978). Monteith (1995) characterized the response of g_s to D as consisting of two different regimes: (i) regime A—where g_s gradually declines with D, but transpiration (E) increases with D and (ii) regime B—where g_s declines non-linearly with D, resulting in a peak and then decline in E. Regime A is the most commonly observed pattern and occurs at intermediate D (0.5–2 kPa). It also represents the range of leaf level measurements most commonly used to parameterize models of g_s (e.g., Ball et al. 1987, Leuning 1995, Medlyn et al. 2011). Regime B takes place at higher D (D >2 kPa), which is typically rare in humid ecosystems but common in hot and dry ones (e.g., Franks et al. 1997, Thomas and Eamus 1999, MacFarlane et al. 2004, Whitley et al. 2013, Gimeno et al. 2018, Renchon et al. 2018).

Current representations of g_s in terrestrial biosphere models (TBMs) differ in their sensitivity to D, especially at D >2 kPa (i.e., regime B; De Kauwe et al. 2015, Knauer et al. 2015, Franks et al. 2017), which has carry-over effects on TBM predictions at high D. The g_s model of Leuning (1995) has a strong D dependence (g_s depends on the reciprocal of D), which yields a reduction in E at high D. However, it can be difficult to parameterize the Leuning model such that it can fit data at both high and low D (Duursma et al. 2014). The parameter values most commonly used are biased towards low D (e.g., those used in the Community Atmosphere Biosphere Land Exchange (CABLE) land surface model (Kowalczyk et al. 2015) or the Sheffield Dynamics Global Vegetation Model (Woodward et al. 1995)). Alternatively, Medlyn et al. (2011) proposed an optimality model, in which g_s depends on $D^{-0.5}$. Due to this lower sensitivity of g_s to D compared with the Leuning model, the Medlyn model does not predict a reduction in E at high D (i.e., regime B).

The reduction of E at high D in regime B could result from a hydraulic limitation (Buckley 2005). Experimental observations show that g_s is strongly linked to guard cell and epidermal turgor (e.g., Franks et al. 1997, Franks 2004) and not simply to environmental conditions (i.e., D). Tuzet et al. (2003) proposed a model coupling g_s to leaf water potential (ψ_L). The ψ_L term in the Tuzet model is determined by the balance of plant water use via stomata and the water supply, which is calculated as the product of hydraulic conductance and the difference between leaf and soil water potentials. In the Tuzet model, ψ_L is solved iteratively by balancing the demand and supply. If the hydraulic conductance is held constant, the Tuzet model will not yield a decline in transpiration at high D because a reduction in ψ_L cannot occur at the same time as a reduction in transpiration (Farquhar 1978). However, reductions in hydraulic conductance can occur within the xylem by cavitation (Tyree and Sperry 1989) or outside the xylem component of the pathway via a variety of mechanisms (Scoffoni et al. 2017). A very negative ψ_L leads to a large pressure difference but low conductance, the net effect of which can lead to a reduction in water supply and thus a decrease in g_s. Although theoretically plausible, the hydraulic limitation hypothesis has not been extensively tested against observations.

An alternative hypothesis to explain the coupled A–g_s response at high D is a non-stomatal limitation of A (Dewar et al. 2017; Gimeno et al. 2019). The mechanism for such a non-stomatal limitation is not clear, but it could potentially involve biochemical regulation or a reduction in mesophyll conductance. For example, Duursma et al. (2014) proposed that the reduction of E at high D is driven by a decrease in apparent carboxylation capacity (V_{cmax}) at the high temperatures (>30 °C) that accompany high D. This hypothesis was supported by leaf- and canopy-scale measurements in a whole-tree chamber experiment (Duursma et al. 2014). Low leaf water potential at high D could also reduce apparent photosynthetic capacity via a downregulation of the capacity of photosynthetic biochemistry or a reduction in mesophyll conductance (Tezara et al. 1999, Lawlor and Cornic 2002, Lawlor and Tezara 2009), which would subsequently drive a coupled reduction in g_s. Such an effect is increasingly reported in soil drought studies (e.g., Zhou et al. 2013, 2014, Verhoef and Egea 2014, Drake et al. 2017). Incorporating a non-stomatal limitation into TBMs has led to improved predictions of soil drought responses (Keenan et al. 2010, Verhoef and Egea 2014, De Kauwe et al. 2015, Drake et al. 2017). Although these studies have shown the importance of non-stomatal limitation under soil drought (i.e., via reduced photosynthetic capacity), it is unclear whether high D can cause the same non-stomatal limitation.

Here, we evaluate alternative stomatal modelling approaches at a woodland site where D reaches high levels every summer (mean daily maximum = 2.7 kPa; maximum = 8 kPa). We first test leaf-scale models against in situ observations that showed a reduction in g_s and A with increasing D (Gimeno et al. 2015). We then implement the best model into a canopy scale model against whole-tree-scale sap flow data that showed a decrease in transpiration at high D (Gimeno et al. 2018). We aim to quantify how well the alternative gas exchange models captured the high D responses of both g_s and A.

Materials and methods

We tested five leaf-scale g_s models in this study (Table 1): (i) the Medlyn model (Medlyn et al. 2011), which is derived from optimal stomatal theory and assumes that g_s depends on the reciprocal of $D^{0.5}$; (ii) the Leuning model (Leuning 1995), which has a similar functional form to the Medlyn model but assumes a stronger g_s sensitivity to D; (iii) the Tuzet stomatal model (Tuzet et al. 2003), which assumes a g_s sensitivity to ψ_L, incorporating a reduction of hydraulic

Table 1. Summary of model parameter values and performance considered in this study. A complete list of parameter and variable values and destination is in Tables S1. Note the differences in meanings and units in g_1 amongst models. Table shows both the coefficient of determination (R^2; higher is better) and inverse of Bayesian information criterion (BIC; lower is better) of both A and g_s. Each criterion is ranked for the best two model combinations (best and second best marked as dark and light shade). Units for parameters are as follows: $g_{1.max}$ and g_{1T}, $kPa^{0.5}$; β, unitless; D_0, kPa; ψ_f and ψ_{fv}, MPa; s_f and s_{fv}, MPa^{-1}; K_{max}, $\mu mol\ m^{-2}\ s^{-1}\ MPa^{-1}$; c_D, kPa^{-1}

g_s models	V_{cmax}/K_{max} model	Fitted parameters	R^2 of A	R^2 of g_s	−BIC
Medlyn (Eq. 1)	V constant	$g_{1.max} = 5.34$ $\beta = 1.34$	0.54	0.62	2452
Leuning (Eq. 2)	V constant	$g_{1.max} = 19.90$ $\beta = 0.38$ $D_0 = 0.72$	0.70	0.76	2411
Tuzet (Eq. 3)	V constant $K = f(\psi_L)$ (Eq. 6)	$g_{1T} = 8.95$ $\psi_f = -4.25$ $s_f = 2.28$ $K_{max} = 1.01$	0.77	0.71	2387
Tuzet (Eq. 3)	$V = f(\psi_L)$ (Eq. 8)	$g_{1T} = 12.83$ $\psi_f = -1.56$ $s_f = 16.62$	0.65	0.75	2397
	$K = f(\psi_L)$ (Eq. 6)	$K_{max} = 3.98$ $\psi_{fv} = -3.42$ $s_{fv} = 0.50$			
Medlyn (Eq. 1)	$V = f(D)$ (Eq. 9)	$g_{1.max} = 5.67$ $\beta = 0.56$ $c_D = 0.14$	0.77	0.74	2384

conductance with low ψ_L (hereafter referred as Tuzet K-PSI); (iv) the Tuzet stomatal model incorporating a non-stomatal limitation at low ψ_L (hereafter referred as Tuzet V-PSI); and (v) the Medlyn model, incorporating a non-stomatal limitation that increases with increasing D (hereafter referred as Medlyn V-D). The comparison between the performance of Medlyn and Leuning model tests whether increasing the sensitivity of g_s to D improves model performance. The Tuzet K-PSI model was chosen to test whether considering a hydraulic limitation improved model performance. The comparison between the Tuzet V-PSI and Medlyn V-D models was designed to test whether this assumption was necessary to improve predictions at high D and to explore the best way to represent non-stomatal limitation.

Data and Materials Availability

The code and parameters of the models are freely available via https://github.com/Jinyan-Yang/Yang_2019_VPD.

Sites

Data were obtained from two sites in the Cumberland Plain Woodland. The first site is the *Eucalyptus* Free-air-CO_2-Enrichment (EucFACE) site in Richmond, Western Sydney, Australia (33.62°S, 150.73°E). The site is a natural mature woodland, dominated by *Eucalyptus tereticornis*. EucFACE consists of six circular plots (referred to as 'rings' hereafter), each of which has a diameter of 25 m (Gimeno et al. 2015). The rings receive two CO_2 concentrations: ambient (rings 1, 4, 5; ambient $CO_2 \approx 400$ µmol mol^{-1}) and elevated (rings 2, 3, 6; ambient CO_2 + 150 µmol mol^{-1}). The data from the elevated CO_2 rings were included in this study to increase the number of observations for statistical testing, but responses to elevated CO_2 are not a focus of the study (see Gimeno et al. 2015, 2018 for analysis of effects of elevated CO_2). Meteorological data measured at EucFACE during the measurement period of the year 2013 are shown in Figure S1 available as Supplementary Data at *Tree Physiology* Online. The second site is 10 km south of EucFACE in the Castlereagh Nature Reserve, Sydney, Australia (33.39°S, 150.46°E) (Zeppel et al. 2008). This site is also a mature natural woodland with *Eucalyptus parramattensis* as the dominant species, a local species closely related to *E. tereticornis*.

Measurements

This study used three types of data: leaf gas exchange (Zeppel et al. 2008; Gimeno et al. 2015), xylem vulnerability curves and sap flow (Zeppel et al. 2008, Gimeno et al. 2018). Leaf gas exchange and xylem cavitation data were used in parameterization as well as evaluation of the g_s models. Sap flow data were used in whole-tree-scale evaluations to test transpiration predictions of the canopy scale model.

Diurnal leaf gas exchange measurements were made throughout the day under prevailing field conditions using LiCOR 6400XT at EucFACE in 2013 (Gimeno et al. 2015) and a LCpro+ system (ADC BioScientific, Hoddesdon, UK) at Castlereagh in 2006 (Zeppel et al. 2008). Canopy access at

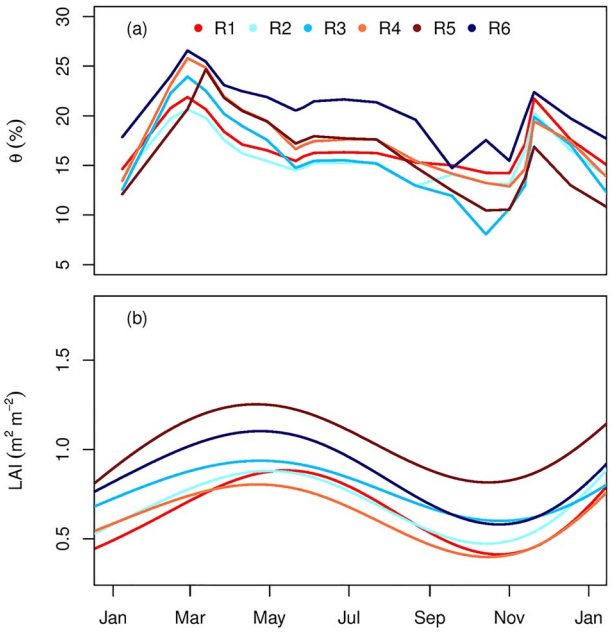

Figure 1. (a) Soil water content (θ; dimensionless) averaged over the top 150 cm of each ring and (b) leaf area index (LAI) at EucFACE in 2013. The LAI data were estimated by Duursma et al. (2016) from measurements of solar radiation transmittance and smoothed with a generalized additive model. Warm (red, orange and brown) and cold (blue, cyan and navy blue) colours depict elevated and ambient CO_2 rings.

EucFACE was provided by a crane (canopy height = 20 m), whereas canopy access at Castlereagh was provided by a portable rising work platform (canopy height = 2–8 m), both suitable to reach the upper canopy. The EucFACE data were measured at saturating photosynthetically active radiation (1800 µmol m^{-2} s^{-1}). The Castlereagh data were measured at ambient light levels, so we only used data with saturating light (>1200 µmol m^{-2} s^{-1}). At EucFACE, leaf water potential measurements at pre-dawn, morning (9:30–11:30h) and afternoon (13:00–15:00h) were also made by Gimeno et al. (2016).

In addition to the four diurnal gas exchange campaigns at EucFACE, repeated light- and temperature-controlled photosynthesis-CO_2 response (A–C_i) curves on the same three or four trees in each ring were measured and used to calculate the maximum apparent electron transport rate (J_{max}; µmol m^{-2} s^{-1}) and apparent carboxylation capacity (V_{cmax}; µmol m^{-2} s^{-1}). The J_{max} and V_{cmax} values were estimated with the 'fitacis' function from the *plantecophys* R package (Duursma 2015). The temperature dependencies of J_{max} and V_{cmax} were obtained from a different set of A–C_i curves measured at four leaf temperatures ranging between 20 and 40 °C during February 2016. We fitted peaked Arrhenius functions to the values of J_{max} and V_{cmax} obtained at each measurement temperature (Medlyn et al. 2002). The resulting J_{max} and V_{mcmax} at 25 °C (i.e., $J_{max.25}$ and $V_{cmax.25}$) values were averaged for each ring on each measurement date. We also estimated one-point V_{cmax} from the diurnal measurements using the 'one-point method' (De Kauwe et al. 2016). As a result, each diurnal gas exchange measurement corresponded to a modelled V_{cmax} based on A–C_i curve data and the temperature response, and an in situ V_{cmax} based on the 'one-point method'.

A hydraulic vulnerability curve for *E. tereticornis* was constructed using benchtop dehydration (Sperry et al. 1988). Two-metre long branches were excised from six mature canopy trees located outside the rings at EucFACE, using the canopy crane. Collections were made in the early morning (between first light and sunrise). Branches were placed in large plastic bags with moist towels to prevent dehydration, and cut ends were recut under water and allowed to rehydrate. Branches were transported in water and were stored in a cool room 24 h before measurements. Stem percent loss of conductivity (PLC) was measured using hydraulic flow measurements on increasingly dehydrated branch segments using a flowmeter (Liqui-Flow L10, Bronkhorst High-Tech BV, Ruurlo, Gelderland, The Netherlands) at low pressure (<4 kPa). Four to six stem segments were measured per large branch at progressively lower water potentials (measured on covered leaves using a pressure chamber—PMS Instrument Company, Albany, OR, USA). To quantify the impact of cavitation for the Tuzet models, a Weibull function following Ogle et al. (2009) was fitted to produce a vulnerability curve using the 'fitplc' function in the *fitplc* R package (Duursma and Choat 2017).

Canopy transpiration was estimated with sap flow measurements at both the EucFACE and the Castlereagh sites. At EucFACE, two custom-built two-probe heat-pulse sensors (Edwards Industries, Havelock North, New Zealand) were installed at two positions on each tree, on three or four trees per ring (Gimeno et al. 2018). The data from all six rings were upscaled to estimate stand averages using sap wood area, which was allometrically calculated with measured stem diameter. The volumetric soil water content (θ) of the site was measured every ~20 days using neutron measurements at 25 cm intervals (NMM, 503DR Hydroprobe®, Instroteck, Research Triangle, NC, USA) and averaged to the mean moisture of the top 150 cm of the soil (Figure 1, Gimeno et al. 2018). Sap flow at the Castlereagh site was obtained from Zeppel et al. (2008). The measurements used two-probe heat-pulse sensors and sampled six trees with two sensors per tree from June to December 2006. The corresponding soil moisture measurements at Castlereagh were recorded with an array of frequency domain reflectometry sensors (Theta Probe, ML2-X; Delta-T devices, Cambridge, UK) for the top 70 cm.

Leaf gas exchange models

We used the Medlyn model as our baseline stomatal conductance model because it requires the fewest parameters (Medlyn et al. 2011):

$$g_s = 1.6 \cdot \left(1 + \frac{g_{1.MED}}{\sqrt{D}}\right) \cdot \frac{A}{C_a} \quad (1)$$

where g_s is the stomatal conductance to water vapour (mol m^{-2} s^{-1}); $g_{1.MED}$ is the optimal stomatal behaviour parameter ($kPa^{0.5}$; see detailed explanation in Medlyn et al. (2011)); A is the CO_2 assimilation rate (μmol m^{-2} s^{-1}); C_a is the atmospheric CO_2 concentration (μmol mol^{-1}). We modelled A with the *plantecophys* R Package (Duursma 2015), which uses the Farquhar-von Caemmerer–Berry photosynthesis model (Farquhar et al. 1980).

An earlier g_s model was proposed by Leuning (1995), who assumed an inverse stomatal response to D:

$$g_s = 1.6 \cdot g_{1.LEU} \cdot \frac{A}{C_a} \cdot \frac{1}{1 + D/D_0} \quad (2)$$

where $g_{1.LEU}$ is an empirical slope determining the sensitivity of g_s to A and other environment variables (dimensionless) and D_0 reflects the sensitivity of g_s to D (kPa). Both the Medlyn and Leuning models can include a minimum stomatal conductance, g_0, as an intercept (Duursma et al. 2019). This study assumed $g_0 = 0$ since the estimated g_0 is negligible (Gimeno et al. 2015).

We also tested a modified version of the model proposed by Tuzet et al. (2003), following Duursma and Medlyn (2012):

$$g_s = 1.6 \cdot g_{1.TUZ} \frac{A}{C_a} \cdot f_s(\psi_L) \quad (3)$$

where $g_{1.TUZ}$ is an empirical slope parameter and f_s is the sigmoidal function defined as:

$$f_s(\psi_L) = \frac{1 + \exp(s_f \cdot \psi_f)}{1 + \exp(s_f \cdot (\psi_f - \psi_L))} \quad (4)$$

where ψ_L is leaf water potential (MPa), ψ_f is an empirical reference water potential (MPa), and s_f is a sensitivity parameter describing the steepness of the response of g_s to ψ_f (MPa^{-1}). The Tuzet model resembles the Medlyn and Leuning models but replaces the dependence on D with a function of ψ_L.

The leaf water potential ψ_L is obtained as follows. Assuming that the transpiration is a balance of demand and supply:

$$E = K \cdot (\psi_s - \psi_L) = g_s \cdot D / P_{atm} \quad (5)$$

where K is the soil-to-leaf hydraulic conductance (mol m^{-2} s^{-1} MPa^{-1}), ψ_s is the soil water potential (MPa), and P_{atm} is the atmospheric air pressure (kPa). To solve for ψ_L requires a value for K, which is assumed to decrease as plant water potential becomes more negative (Tyree and Sperry 1989):

$$K = K_{max} \cdot R_{PLC} \quad (6)$$

where K_{max} is the maximum hydraulic conductance (μmol m^{-2} s^{-1} MPa^{-1}). R_{PLC} is the percentage loss of hydraulic conductance and takes the form of a Weibull function as fitted by Neufeld et al. (1992):

$$R_{PLC} = \frac{1}{1 + \exp(a \cdot (\psi_L - \psi_{50}))} \quad (7)$$

where a and ψ_{50} are fitted parameters, representing the rate of decline of the curve and the leaf water potential at which plant hydraulic conductance is reduced to 50%, respectively. This equation was fitted to the hydraulic vulnerability curves described above. Combining Eqs (3)–(7) allows both ψ_L and g_s to be predicted.

We tested two alternative ways to represent non-stomatal limitations. In the first, V_{cmax} was assumed to decline with leaf water potential (the V-PSI hypothesis):

$$V = V_{cmax} \frac{1 + \exp(s_{fv} \cdot \psi_{fv})}{1 + \exp(s_{fv} \cdot (\psi_{fv} - \psi_L))} \quad (8)$$

where V is the V_{cmax} modified by non-stomatal limitation and s_{fv} and ψ_{fv} are fitted parameters. ψ_{fv} is an empirical reference water potential (MPa), and s_{fv} is a sensitivity parameter describing the 'steepness' of the response of V_{cmax} to ψ_{fv} (MPa^{-1}). Note that this is the same form of sigmoidal function as used in the Tuzet model (Eq. (3)).

In the second representation of the non-stomatal limitation, we derived a direct empirical relationship between V_{cmax} and D (the V-D hypothesis):

$$V = \min(10, V_{cmax} \cdot (1 - c_D \cdot D)) \quad (9)$$

where c_D is a fitted parameter (kPa^{-1}). This relationship is different from that in Eq. (8) because it assumes the apparent carboxylation capacity directly responds to D. Although the mechanism for such a change is unclear, this simple empirical approach allows us to explore the possibility of direct down-regulation of apparent V_{cmax} and J_{max}. Similar simple empirical approaches have been used to explore non-stomatal limitation under low soil moisture content (e.g., Keenan et al. 2010, Verhoef and Egea 2014, De Kauwe et al. 2015, Drake et al. 2017). We set a minimum V_{cmax} of 10 (μmol m^{-2} s^{-1}) to avoid negative values produced by the linear decline of V_{cmax} with D. The same relationship is assumed for J_{max}.

We assumed that the impact of reduced soil water availability could be represented in the Tuzet model by the reduction of soil moisture potential (ψ_s), which was estimated from the pre-dawn leaf water potential (ψ_{pd}; MPa). For the Medlyn and Leuning

models, we assumed an exponential dependence of the g_1 parameter on ψ_{pd} following Zhou et al. (2013):

$$g_1 = g_{1.MAX} \cdot \exp\left(\beta \cdot \psi_{pd}\right) \quad (10)$$

where g_1 represents $g_{1.MED}$ and $g_{1.LEU}$; $g_{1.MAX}$ is g_1 when $\psi_{pd} = 0$ and β represents the sensitivity of g_1 to ψ_{pd}. The impact of dry soil was implemented to account for the variation in the soil water availability amongst the campaigns.

Parameterization of leaf gas exchange models

We used R (version 3.4.1, R Development Core Team) as the modelling and statistical tool. We used measured values of incident photosynthetically active radiation, leaf temperature, atmospheric CO_2 concentration, D, ψ_{pd}, J_{max}, and V_{cmax} for the diurnal gas exchange data (at EucFACE only). We then parameterized the Medlyn and Leuning models at leaf scale using the differential evolution algorithm (*DEoptim* package) to fit all the parameters ($g_{1.MAX}$, β, D_0, and c_D) in the coupled A–g_s model against the measured A and g_s data. We used a similar approach to determine the unknown parameter values in the Tuzet models. As a result, all the models tested at the leaf-scale were fitted to measurements of A and g_s.

The fidelity of the leaf-scale models was evaluated via: (i) the Bayesian Information Criteria (BIC), which considered the relative residuals of predictions (both A and g_s) as well as the number of parameters in the models; and (ii) the coefficient of determination (R^2) of both A and g_s. We ranked the models with these measures and selected the one with the highest overall ranking.

Stand scale model

We implemented the Medlyn model (Eq. (1)) with V-D relationship (Eq. (9)) into a process-based stand-scale model MAESPA (Duursma and Medlyn 2012). For the purposes of this study, the plant hydraulics sub-model of MAESPA was not used; instead soil water content was prescribed rather than being simulated. The stand simulation included all six rings in EucFACE and covered the period between 1 January 2013 and 31 December 2013 on a half-hourly basis. MAESPA considers the radiative transfer to an array of grid points within each tree crown and calculates gas exchange at each grid point based on light interception at each timestep. Understory plants were not included here because they do not contribute to tree transpiration. The model was parameterized with data on size and position of each tree as well as the smoothed and gap-filled leaf area index (Duursma et al. 2016, Figure S1) available as Supplementary Data at *Tree Physiology* Online.

Meteorological (Figure S1 available as Supplementary Data at *Tree Physiology* Online) and soil water content data (Figure 1) observed in each ring were the input to the model. The original met data were aggregated to half-hourly averages and gap-filled with nearest available values (<1% of the total). Canopy physiology was parameterized with measurements of the light response of photosynthesis, dark respiration rate, and the temperature response of photosynthesis and respiration, all made at EucFACE and assumed not to vary across treatments. We assumed a minimum g_s (Duursma et al. 2019) of 0.01 (mol H_2O m^{-2} leaf s^{-1}) during daytime to avoid zero transpiration at extreme environmental conditions (e.g., high D). The transpiration of the canopy in the model is given by the Penman–Monteith equation, which considers net radiation, windspeed, relative humidity and g_s.

The impact of low soil water content on stomatal conductance in MAESPA was modelled as a function of g_1 and volumetric soil water (θ) content following Drake et al. (2017):

$$g_1 = g_{1.SAT} \cdot \left(\frac{\theta - \theta_{min}}{\theta_{max} - \theta_{min}}\right)^q \quad (11)$$

where $g_{1.SAT}$ is the value of g_1 ($kPa^{0.5}$) at saturating soil water content; θ_{max} and θ_{min} are empirically fitted parameters defining the upper and lower boundaries beyond which g_1 is not affected by θ and q is the parameter describing the non-linearity of the function. We fitted Eq. (11) to the data from Gimeno et al. (2015) to obtain the values of θ_{max}, θ_{min} and q (0.25, 0.11 and 0.38, respectively) with the non-linear least squares method (nls, R function). The fitted relationship between $g_{1.MAX}$ and θ used in the model is shown in Figure S2 available as Supplementary Data at *Tree Physiology* Online. J_{max} in MAESPA is taken as a constant mean of 159 (μmol m^{-2} s^{-1}) for all rings and time. V_{cmax} in MAESPA also remained constant over time but taken as 83 (μmol m^{-2} s^{-1}) for elevated CO_2 rings and 91 for ambient CO_2 rings as per measurements (Ellsworth et al. 2017, Wujeska-Klause et al. 2019). The parameter values used in MAESPA are presented in Table S2 available as Supplementary Data at *Tree Physiology* Online.

Results

Leaf gas exchange models

The leaf gas exchange data from EucFACE showed a clear decline in both A and g_s with increasing D (Figure 2). The baseline model (Medlyn with constant V) was unable to capture the response of A (Figure 3a) or g_s (Figure 3b) to D. As a result, this model ranked lowest amongst the models tested (BIC = −2452; Table 1). It over-predicted A at high D but under-predicted g_s at low D. The Leuning model, despite its stronger sensitivity to D, shared the same problems as the Medlyn model (Table 1, Figure 3c and d). In addition, we obtained unrealistic parameter values ($g_{1.MAX}$, β, and D_0) for the Leuning model (Table 1). Utilizing the default parameter values for the Leuning model used in the CABLE land-surface model (for the evergreen broadleaf plant functional type), for example, led to severe under-prediction of g_s (Figure S3 available as Supplementary Data at *Tree Physiology* Online). In other words, with commonly

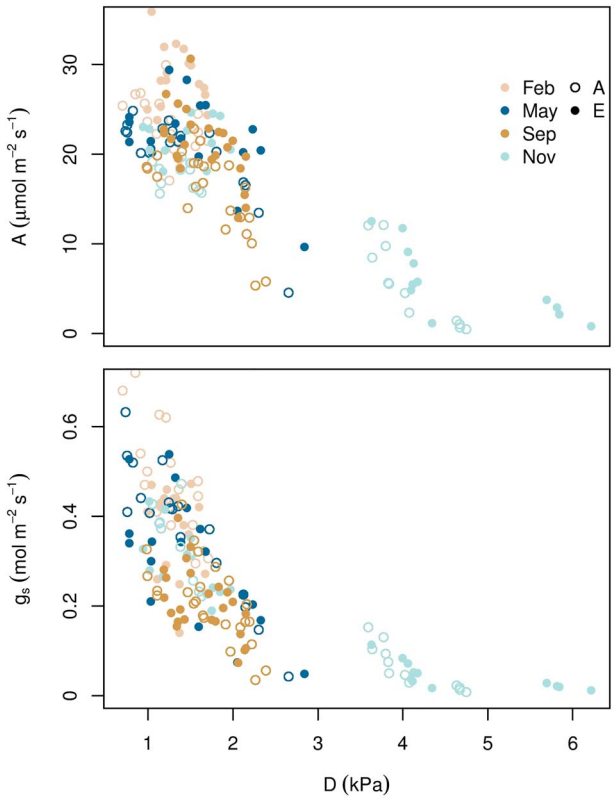

Figure 2. The observed response of light-saturated photosynthesis (A) and stomatal conductance (g_s, re-drawn from Gimeno et al. 2015) to vapour pressure deficit (D) in the Licor chamber at EucFACE. Data are leaf gas exchange from four campaigns in 2013 in all six rings (obtained from Gimeno et al. 2015). The chamber D is similar to that of the outside air. Open circles: ambient (A) rings; closed circles: elevated (E) rings.

used parameter values, the Leuning model would have performed worse than all other models tested here (BIC = −2479).

The model incorporating hydraulic limitation (Tuzet K-PSI) showed a good agreement (BIC = −2387) with observations at both low and high D (Figure 4 and Table 1). It achieved the second-best BIC value (Table 1). However, a comparison with the measured leaf water potential values shows that the Tuzet model performed well for the wrong reasons. The Tuzet K-PSI model predicted a decline of ψ_L with increasing D (Figure 5a), a large gradient between ψ_s and ψ_L (~4 MPa), and ψ_L values below ψ_{50} (<−5 MPa). None of these predictions was supported by the observations (Figure 5). The observed ψ_L did not change with D (Figure 5a) and remained above the point of onset of embolism in all measurements (Figure 5b). The minimum observed ψ_L value was −3.3 MPa, which was estimated to correspond to a PLC of 18%.

We examined the gas exchange data directly for evidence of non-stomatal limitation. Figure 6 shows the ratio of one-point V_{cmax} (estimated from gas exchange data using the 'one-point' method) to the predicted V_{cmax} at the same temperature (estimated from A–C_i curves performed at a range of temperatures). This ratio declined strongly with increasing D as shown by data from EucFACE and Castlereagh sites. This decline in the one-point V_{cmax} clearly demonstrates that non-stomatal limitation is a factor in the decline of A at high D.

We then tested whether the non-stomatal limitation could be predicted as a function of leaf water potential (Tuzet V-PSI). Adding non-stomatal limitation to the Tuzet model comes at a cost of increased complexity, requiring six parameters to be fitted at the same time. This added complexity was not justified by the marginal improvements in R^2 resulting in the worst BIC value of all models tested (Table 1, Figure 7a and b). Including the non-stomatal limitation in the Tuzet model did not lead to model improvement, which can be explained as follows. First, we know that the plants did not reduce ψ_L sufficiently to cause cavitation and a reduction in hydraulic conductance (Figure 5). Therefore, the non-stomatal limitation as a function of ψ_L cannot predict a reduction in transpiration at high D. The observed decrease in g_s at high D leads to a less negative ψ_L at high D, and a less negative ψ_L implies a higher V_{cmax}. Higher V_{cmax} at high D contradicts both the assumption of non-stomatal limitation and the evidence shown in Figure 6.

Incorporating non-stomatal limitation into the Medlyn model (Medlyn V-D; Figure 7c and d) improved the model predictions of both A and g_s (BIC = −2384). The Medlyn model, together with an empirical decline in V_{cmax} with D, achieved better R^2 values for both A and g_s than the more complicated models, resulting in the best BIC value (Table 1).

It is not possible to determine from our measurements what mechanism causes this reduction in apparent V_{cmax}. Following Zhou et al. (2013), we investigated the possibility that the reduction is largely attributable to a reduction in mesophyll conductance by estimating how large the reduction in mesophyll conductance (gm) would need to be, to fully explain the observed reduction in one-point V_{cmax}. We assumed that all the discrepancy between the Medlyn model prediction and diurnal gas exchange data could be attributed to g_m. Then, for each diurnal measurement, a g_m value was estimated as that which minimized the difference between the model predictions and the diurnal observations. A reduction in g_m from 0.2 to 0.01 mmol m^{-2} s^{-1} would be implied if non-stomatal limitations were entirely due to a reduction of g_m (Figure 8).

Stand scale model

Whole-tree transpiration estimated from sap flow measurements was used to evaluate the performance of the Medlyn V-D hypothesis at the whole-tree scale using the MAESPA model. The standard MAESPA using the Medlyn model overpredicted transpiration at EucFACE especially at high D (example of ring 2 in Figure 9a and b). The difference between the predicted and observed values increased strongly at high D (compare green with red dots in Figure 9b). However, after incorporating the Medlyn V-D model, MAESPA closely followed the seasonal

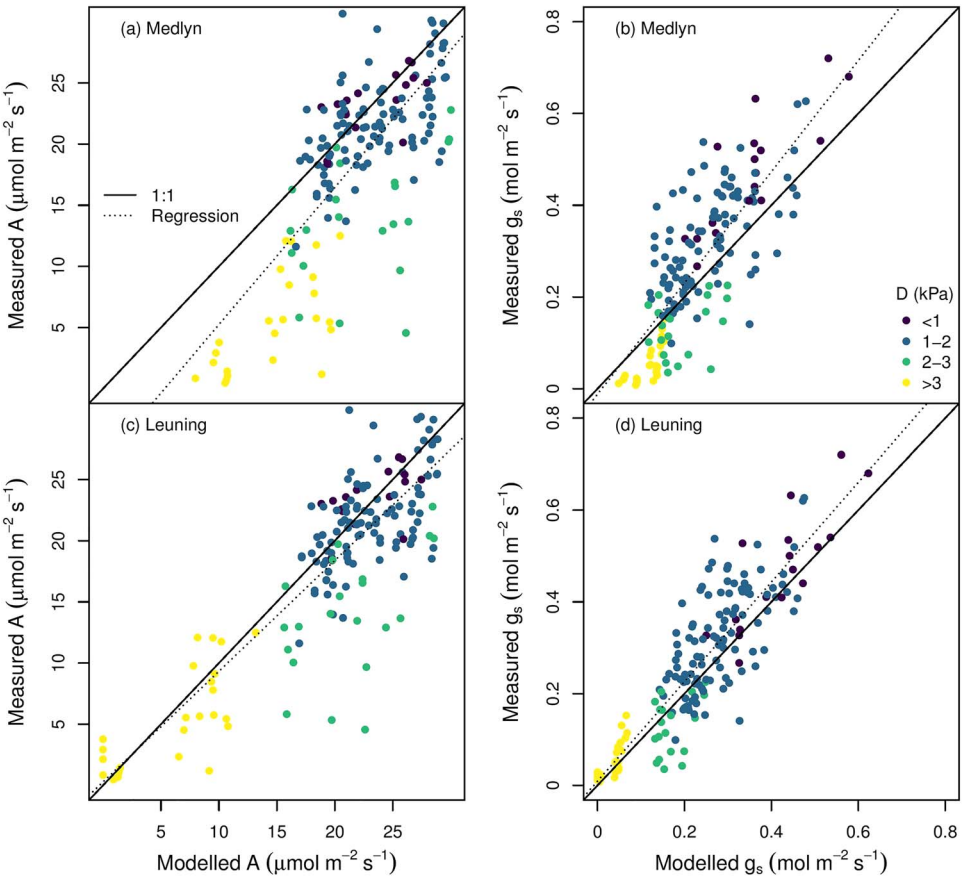

Figure 3. Modelled photosynthesis (A) and stomatal conductance (g_s) compared with observations. (a and b) Medlyn model (Eq. (1)). (c and d) Leuning model (Eq. (2)). Models were fitted to both A and g_s data.

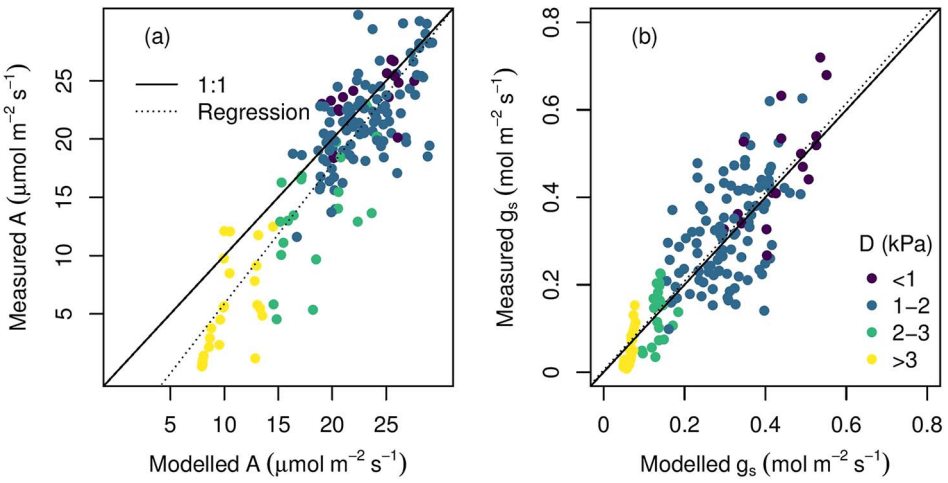

Figure 4. Modelled photosynthesis (A) and stomatal conductance (g_s) incorporating hydraulic limitation (Tuzet K-PSI, Eqs (3)–(7)) compared with observations.

variation of the measurements (Figure 7c) and agreed with observations across the full range of D. Overall, incorporating the Medlyn V-D model increased the coefficient of determination from 0.78 to 0.87 and reduced the root mean squared error (0.027 to 0.025; l h^{-1}). The improvements were even larger at high D (>2.5 kPa), with a reduction of root mean squared error from 0.070 to 0.037. During the simulated year of 2013, incorporating non-stomatal limitation into MAESPA, resulted in a ~19% reductions in predicted annual transpiration (59.7 kg H_2O m^{-2} $year^{-1}$) and a ~14% reduction in gross primary production (222.4 g C m^{-2} $year^{-1}$). These findings indicate a large impact of non-stomatal limitation at high D.

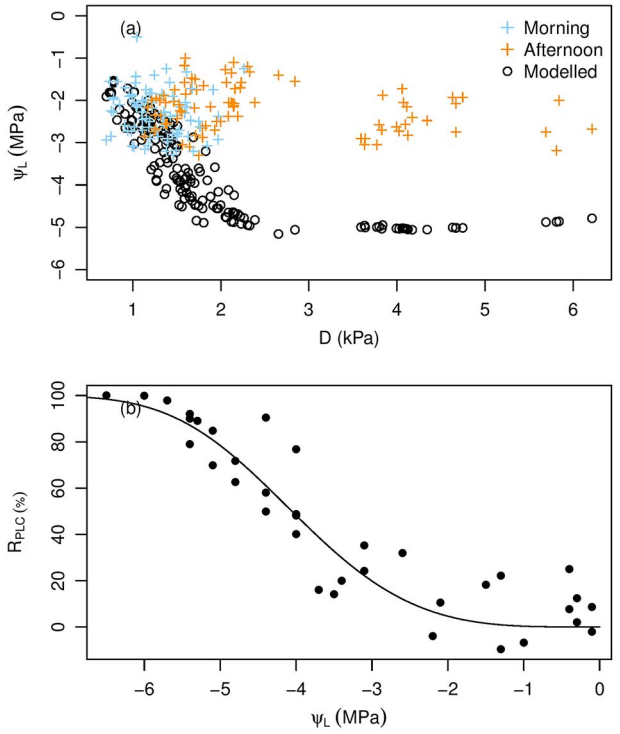

Figure 5. The Tuzet K-PSI model did not capture the observed leaf water potential (ψ_L). (a) Predicted and observed ψ_L (circles and crosses, respectively) from the Tuzet model. Observations were made mid-morning (lower *D*, shown in blue) or early afternoon (higher *D*, shown in orange). (b) Estimated PLC curve based on dehydration measurements. Note in (a) that observed ψ_L stays above the water potential corresponding to ~20% PLC (>−3 MPa), but the model predicts this value to fall to ~80% PLC (<−5 MPa).

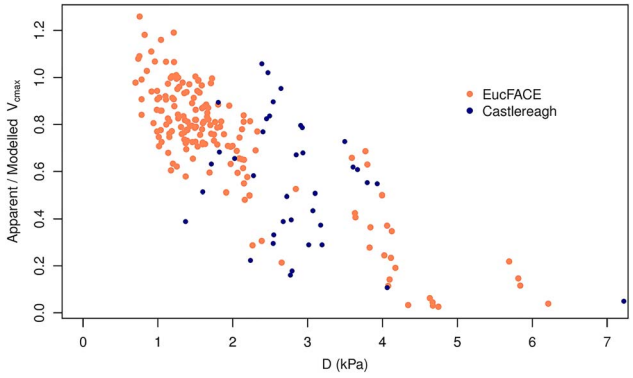

Figure 6. Ratio of one-point V_{cmax} (estimated from gas exchange data using the 'one-point' method) to the predicted V_{cmax} at the same temperature (estimated from *A*-C_i curves performed at a range of temperatures), as a function of *D*. EucFACE data (orange) are from Gimeno et al. (2015); Castlereagh data (blue) are from Zeppel et al. (2008). Only the EucFACE data are used in parameterization; the Castlereagh data are used to show that the pattern is consistent across sites in the area.

We also explored whether the new model would improve predicted transpiration compared with observations at the Castlereagh site with similar species and climate conditions. Without canopy physiology or canopy structure data to parameterize the Castlereagh site, we took the approach of standardizing the observed sap flow and modelled *E* by their respective maxima and comparing the relationships of *E* with *D* (Figure 10). Both sites show a peaked relationship of *E* with *D,* with the turning point occurring between 1 and 3 kPa, which agrees with the prediction of MAESPA incorporating non-stomatal limitation (red line in Figure 10).

Discussion

We evaluated a suite of commonly used g_s models and assumptions (hydraulic and non-stomatal limitation) used to represent the coupled *A*–g_s response to *D* at two native evergreen woodland sites in western Sydney. The observed decline of *A* and g_s at high *D* could not be captured with current widely used models of stomatal conductance, and models were not improved by incorporating hydraulic limitation and xylem cavitation. The model incorporating a non-stomatal limitation (i.e., a reduction of apparent photosynthetic capacity with increasing *D*) gave the best agreement with the observations at a large range of *D*. This finding highlights the importance of accounting for non-stomatal limitation in TBMs.

Standard models

Standard leaf gas exchange models, embedded within TBMs, perform poorly when *D* increases above 2.5 kPa despite their wide use and important role (De Kauwe et al. 2015, Knauer et al. 2015). This finding is in line with previous studies showing the difficulties of modelling leaf gas exchange at high *D* (e.g., Franks et al. 1997, Farquhar 1978, Eamus et al. 2008). Our analysis re-emphasizes the need to improve leaf gas modelling in ecosystems that experience high *D*. The concerned regions include drylands, which cover 41% of the earth's land surface (Reynolds et al. 2007) and potentially tropical, subtropical and temperate ecosystems during dry seasons and heatwaves (Novick et al. 2016).

The comparison between the Leuning (1995) and Medlyn et al. (2011) models yields an important result, which is that improvements in the performance of the leaf gas exchange model at high *D* are unlikely to be achieved by varying the stomatal sensitivity to *D*. The Medlyn model does not have a mechanism that allows g_s or *A* to decrease at high *D* except via the temperature dependence of photosynthesis (Duursma et al. 2014; Kala et al. 2016). In contrast, the Leuning model does have a stronger regulation of g_s at high *D* but performs poorly at low *D* (Figure 3, and Figure S3 available as Supplementary Data at *Tree Physiology* Online) and requires an additional parameter to achieve this compared with the Medlyn model. Nonetheless, neither model is able to capture both g_s and *A* at high *D*.

Models with hydraulic limitation

The decline of g_s at high *D* in the models incorporating hydraulic limitation is achieved either by a small hydraulic conductance

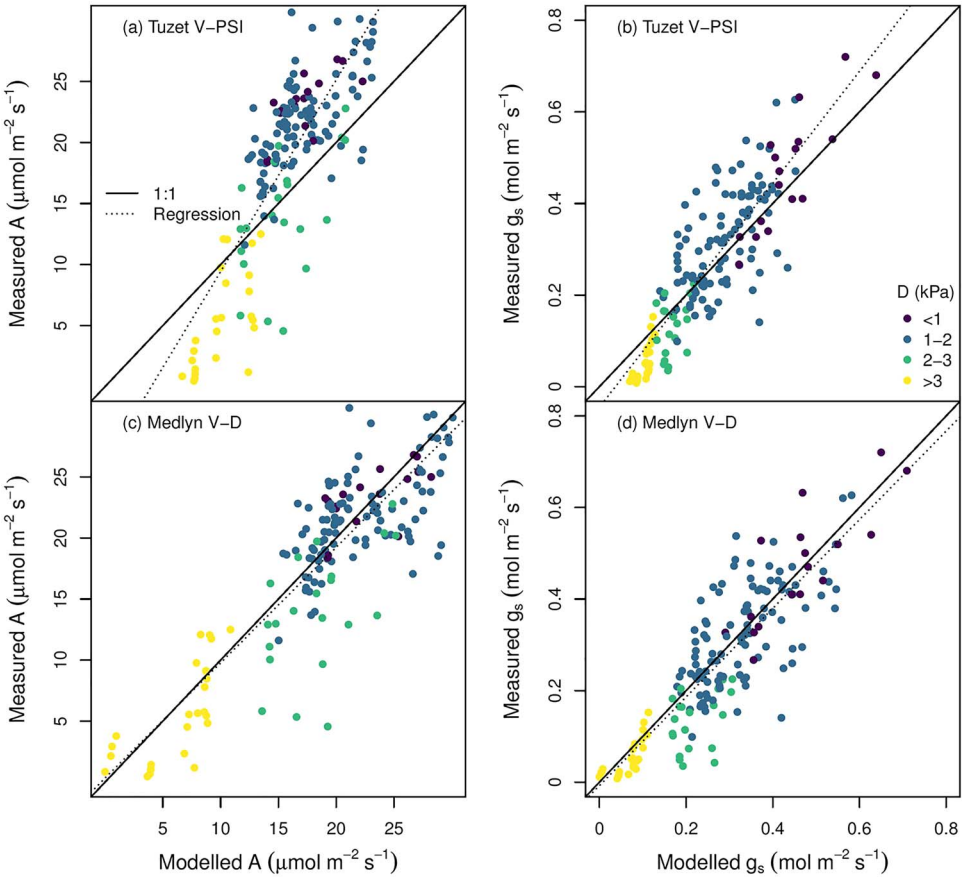

Figure 7. Modelled photosynthesis (A) and stomatal conductance (g_s) incorporating non-stomatal limitation (Eq. (9)) into Tuzet (Tuzet V-PSI) and Medlyn models (Medlyn V-D) compared with observations.

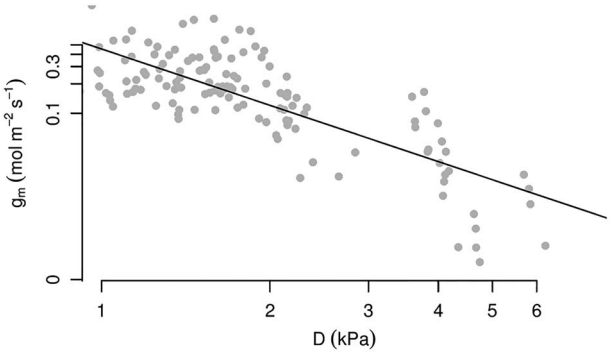

Figure 8. Estimated mesophyll conductance (g_m; mol m^{-2} s^{-1}) shows a decline with increasing vapour pressure deficit (D; kPa). The g_m is estimated from diurnal leaf gas exchange measurements in EucFACE during 2013 under the assumption that the observed decline in V_{cmax} is entirely due to decreasing g_m. The line marks the linear regression fit: $\ln(g_m) = -0.79 - 1.91 \cdot \ln(D)$ with a R^2 of 0.6. The fitting estimates a g_m of 0.12 mol m^{-2} s^{-1} at D = 2 kPa, and 0.03 mol m^{-2} s^{-1} at D = 4 kPa.

(resulting from a very negative ψ_L) or by a small pressure gradient (resulting from a ψ_L close to ψ_S). The Tuzet model assumes the decline of ψ_L drives the reduction of g_s at high D. We found that this assumption led to an unrealistic decline in ψ_L with increasing D, contradicting ψ_L observations, which remained relatively consistent over the course of a day (Figure 5a). Moreover, the predicted ψ_L fell below the estimated ψ_{50}, which is inconsistent with previous studies suggesting plants maintain ψ_L above the point of onset of xylem embolism (Sperry et al. 2002; Choat et al. 2012; Li et al. 2018).

Incorporating non-stomatal limitation allowed a ψ_L close to ψ_S at high D. However, a less negative ψ_L implied a higher V_{cmax} at high D, which again contradicted the assumption of non-stomatal limitation and the observations (Figure 6). As a result, the hydraulic limitation as implemented here was unable to capture the observed D responses. Alternative models could potentially be more successful: Buckley and Mott (2013), for instance, proposed to model stomatal regulation via guard cell osmotic pressure in response to the water status of the surrounding epidermal cells. This approach is important, because it can also incorporate increases in extra-xylary resistance that have been observed to occur in leaves (Yang and Tyree 1994; Scoffoni et al. 2017), roots (Cuneo et al. 2016) and the rhizosphere (North and Nobel 1997). However, at this point, the majority of models do not incorporate these resistances.

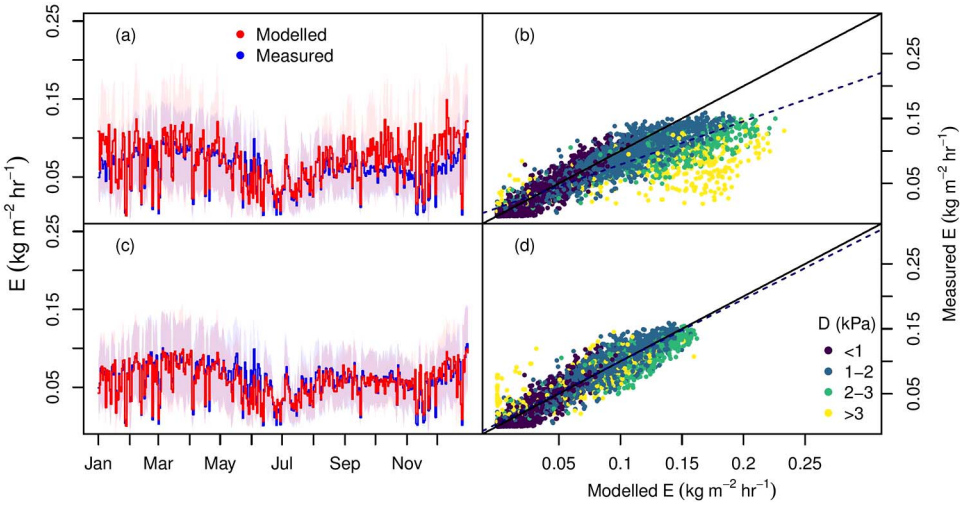

Figure 9. Modelled transpiration (*E*) compared with sap flow estimated by heat pulse sensors (measured *E*). Data shown are daytime for one stand (ring 2) in 2013. Other stands are similar (Figures S4–S8) available as Supplementary Data at *Tree Physiology* Online. Panels (a) and (b) show measured and modelled *E* over time from original MAESPA. Panels (c) and (d) show the result from MAESPA with V-D hypothesis. The solid lines in panels (a) and (c) show the daily average, whilst the shading shows hourly variation (standard deviation).

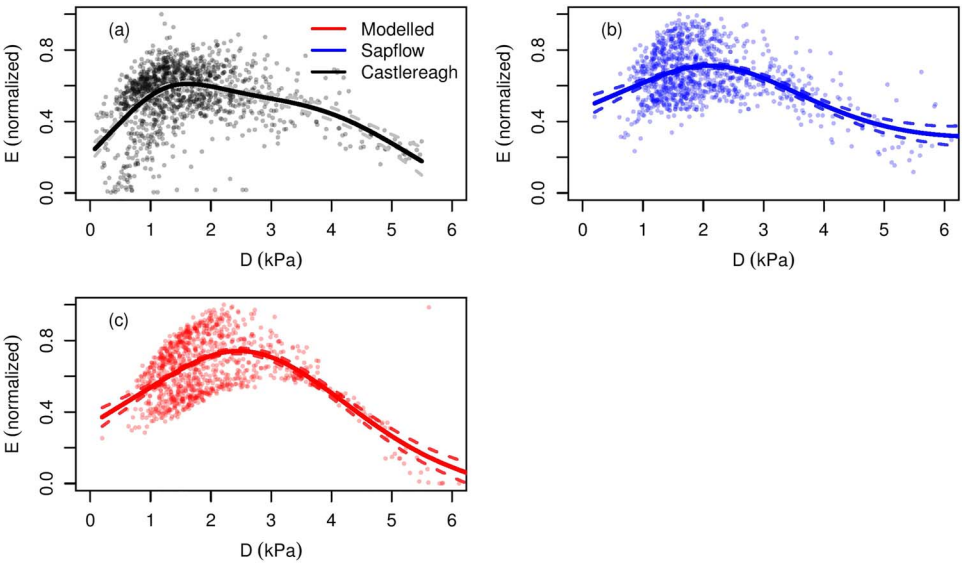

Figure 10. Transpiration (*E*) across different sources/sites as a function of vapour pressure deficit (*D*). (a)Sap flow data from Castlereagh (Zeppel et al. 2008). Bold line: generalized additive model (df = 5) fit to the data at saturated light (with PAR >75% quantile). Panels (b) and (c) are the estimated (sap flow) and modelled half-hourly daytime *E* for ring 2 at EucFACE in 2013, respectively. Black and blue lines represent the same fitting to the modelled and sap flow data.

Plausible mechanisms of non-stomatal limitation

Studies on mesophyll conductance and photosynthetic capacity (e.g., Mediavilla et al. 2002; Nascimento and Marenco 2013) have suggested the importance and mechanisms of non-stomatal limitation. The proposed mechanisms for non-stomatal limitation fall into two categories: (i) a biochemical signalling-induced reduction in carboxylation capacity and (ii) a reduction in mesophyll conductance, both of which have some empirical and theoretical support. Lawlor and Cornic (2002) and Lawlor and Tezara (2009) illustrated that carboxylation capacity is downregulated at high water deficit due to reduction in adenosine triphosphate synthesis. Huang et al. (2006) explored the cause of 'midday depression of g_s and *A*, and suggested that the regulation of photosynthetic capacity is the likely explanation as plants aim to protect chloroplasts.

An alternative explanation for the decline of carboxylation capacity in the afternoon is sink limitation. It has been proposed that the accumulation of starch and sugar in the leaf over time causes an inhibition of photosynthesis (Paul and Foyer 2001). We did not explore this effect because the data do not support

this explanation at EucFACE (Wujeska-Klause et al. 2019). We compared the diurnal time-course of photosynthesis for days with low and high *D* (Figure S9 available as Supplementary Data at *Tree Physiology* Online). On days with low *D*, there is no reduction in afternoon photosynthesis even though morning photosynthesis was high, indicating that the accumulation of starch and sugar is not strong enough to cause a reduction in photosynthetic capacity.

It is also possible that non-stomatal limitation is due to a reduction of (g_m with increasing *D*. Flexas et al. (2008) examined our current understanding of the response of g_m to the environment (including *D*) and suggested that g_s and g_m could be co-regulated. Warren (2008) reported no g_m response to *D* in *Eucalyptus* seedlings. However, that study only considered a small range of *D* (1–2 kPa), which is not sufficient to show the decline observed here. We investigated how large the reduction in g_m would need to be to fully explain the observed reduction in apparent V_{cmax} and found that a reduction in g_m from 0.2 to 0.01 mmol m^{-2} s^{-1} would be implied if non-stomatal limitations were entirely due to a reduction of g_m (Figure 8). These values and magnitude of change of g_m are consistent with previous studies (Niinemets et al. 2009, von Caemmerer and Evans 2015), suggesting that the apparent downregulation could potentially be attributable to g_m. However, this result is not conclusive because we are unable to quantify g_m with the data available.

Consequences for TBMs

This study showed that the current gas exchange models in TBMs can perform poorly at high *D*. Terrestrial biosphere models thus may be improved by incorporating non-stomatal limitation to predict *A* and g_s more accurately at high *D*. Previous studies have recommended using non-stomatal limitation to improve modelled response to decreasing soil moisture availability (e.g., Keenan et al. 2010, Egea et al. 2011; Zhou et al. 2013; De Kauwe et al. 2015). Knauer et al. (2019) further demonstrated that incorporating non-stomatal limitation significantly changed the predicted CO_2 response in TBMs. Here, we suggest that incorporating non-stomatal limitation at high *D* may be necessary to capture the correct diurnal pattern of g_s and *A,* as well as annual transpiration and gross primary production in ecosystems currently experiencing high *D* (>2 kPa) and likely to under future warming.

However, we showed that under current hydraulic limitation assumptions, non-stomatal limitation cannot be successfully linked to ψ_L. We applied a simple empirical relationship to estimate non-stomatal limitation with *D*, but without a good understanding of the underpinning mechanism or its generality, it is unclear how widely this empirical dependence could be used. Further studies at high *D* would be useful to quantify the impact of non-stomatal limitation more broadly and to develop theoretical or mechanistic models (e.g., Gimeno et al. 2019). To inform mechanistic models of non-stomatal limitation, future studies need to collect extensive leaf gas exchange data across plant functional types under high *D* (>2 kPa). In addition, mechanistic studies are needed to elucidate the key processes underlying non-stomatal regulation, including changes in photosynthetic capacity and g_m. The empirical relationship describing non-stomatal limitation that we present here could be replaced with theoretical or mechanistic alternatives as they emerge.

Conflict of interest statement

None declared.

Supplementary Data

Supplementary Data for this article are available at *Tree Physiology* Online.

Acknowledgments

We thank Vinod Kumar, Craig McNamara and Craig Barton, for their excellent technical support. We also thank Elise Dando for help in measuring crown radius.

Funding

J.Y. was supported by a PhD scholarship from Hawkesbury Institute for the Environment, Western Sydney University. M.G.D.K. acknowledges funding from the Australian Research Council (ARC) Centre of Excellence for Climate Extremes (CE170100023), the ARC Discovery Grant (DP190101823) and support from the NSW Research Attraction and Acceleration Program. EucFACE was built as an initiative of the Australian Government as part of the Nation-building Economic Stimulus Package and is supported by the Australian Commonwealth in collaboration with Western Sydney University. It is also part of a Terrestrial Ecosystem Research Network Super-site facility.

References

Ball JT, Woodrow IE, Berry JA (1987) A model predicting Stomatal conductance and its contribution to the control of photosynthesis under different environmental conditions. Prog Photosynth Res 5:221–224.

Buckley TN (2005) The control of stomata by water balance. New Phytol 168:275–292.

Buckley TN, Mott KA (2013) Modelling stomatal conductance in response to environmental factors. Plant Cell Environ 36:1691–1699.

von Caemmerer S, Evans JR (2015) Temperature responses of mesophyll conductance differ greatly between species. Plant Cell Environ 38:629–637.

Choat B, Jansen S, Brodribb TJ, Cochard H, Delzon S, Bhaskar R, Bucci SJ, Feild TS, Gleason SM, Hacke UG, Jacobsen AL, Lens F, Maherali H, Martínez-Vilalta J, Mayr S, Mencuccini M, Mitchell PJ, Nardini A,

Pittermann J, Pratt RB, Sperry JS, Westoby M, Wright IJ, Zanne AE (2012) Global convergence in the vulnerability of forests to drought. Nature 491:752–5.

Cowan IR (1978) Stomatal Behaviour and Environment. In: Advances in Botanical Research 4:117–228.

Cowan IR, Farquhar GD (1977) Stomatal function in relation to leaf metabolism and environment. Symp Soc Exp Biol 31:471–505.

Cuneo IF, Knipfer T, Brodersen CR, McElrone AJ (2016) Mechanical failure of fine root cortical cells initiates plant hydraulic decline during drought. Plant Physiol 172:1669–1678.

De Kauwe MG, Kala J, Lin YS, Pitman AJ, Medlyn BE, Duursma RA, Abramowitz G, Wang YP, Miralles DG (2015) A test of an optimal stomatal conductance scheme within the CABLE land surface model. Geosci Model Dev 8:431–452.

De Kauwe MG, Lin Y, Wright IJ et al. (2016) A test of the 'one-point method' for estimating maximum carboxylation capacity from field-measured, light-saturated photosynthesis. New Phytol 210:1130–1144.

Dewar R, Mauranen A, Mäkelä A, Hölttä T, Medlyn B, Vesala T (2017) New insights into the covariation of stomatal, mesophyll and hydraulic conductances from optimization models incorporating nonstomatal limitations to photosynthesis. New Phytol 1103:1–43.

Drake JE, Power SA, Duursma RA et al. (2017) Stomatal and non-stomatal limitations of photosynthesis for four tree species under drought: a comparison of model formulations. Agric For Meteorol 247:454–466.

Duursma RA (2015) Plantecophys - an R package for analysing and modelling leaf gas exchange data. PLoS One 10:1–13.

Duursma R (2017) fitplc - an R package to fit hydraulic vulnerability curves. J Plant Hydraul 4:002.

Duursma RA, Medlyn BE (2012) MAESPA: a model to study interactions between water limitation, environmental drivers and vegetation function at tree and stand levels, with an example application to [CO_2] $\times$ drought interactions. Geosci Model Dev 5:919–940.

Duursma RA, Barton CVM, Lin YS, Medlyn BE, Eamus D, Tissue DT, Ellsworth DS, McMurtrie RE (2014) The peaked response of transpiration rate to vapour pressure deficit in field conditions can be explained by the temperature optimum of photosynthesis. Agric For Meteorol 189–190:2–10.

Duursma RA, Gimeno TE, Boer MM, Crous KY, Tjoelker MG, Ellsworth DS (2016) Canopy leaf area of a mature evergreen *Eucalyptus* woodland does not respond to elevated atmospheric [CO_2] but tracks water availability. Glob Chang Biol 22:1666–1676.

Duursma RA, Blackman CJ, Lopéz R, Martin-StPaul NK, Cochard H, Medlyn BE (2019) On the minimum leaf conductance: its role in models of plant water use, and ecological and environmental controls. New Phytol 221:693–705.

Eamus D, Taylor DT, Macinnis-Ng CMO, Shanahan S, De Silva L (2008) Comparing model predictions and experimental data for the response of stomatal conductance and guard cell turgor to manipulations of cuticular conductance, leaf-to-air vapour pressure difference and temperature: feedback mechanisms are able to account for. Plant Cell Environ 31:269–277.

Egea G, Verhoef A, Vidale PL (2011) Towards an improved and more flexible representation of water stress in coupled photosynthesis-stomatal conductance models. Agric For Meteorol 151:1370–1384.

Ellsworth DS, Anderson IC, Crous KY et al. (2017) Elevated CO_2 does not increase eucalypt forest productivity on a low-phosphorus soil. Nat Clim Chang 7:279–282.

Farquhar G (1978) Feedforward responses of stomata to humidity. Aust J Plant Physiol 5:787.

Farquhar GD, Caemmerer S, Berry JA (1980) A biochemical model of photosynthetic CO2 assimilation in leaves of C3 species. Planta 149:78–90.

Ficklin DL, Novick KA (2017) Historic and projected changes in vapor pressure deficit suggest a continental-scale drying of the United States atmosphere. J Geophys Res 122:2061–2079.

Flexas J, Ribas-Carbó M, Diaz-Espejo A, Galmés J, Medrano H (2008) Mesophyll conductance to CO_2: current knowledge and future prospects. Plant Cell Environ 31:602–621.

Franks PJ (2004) Stomatal control and hydraulic conductance, with special reference to tall trees. Tree Physiol 24:865–878.

Franks PJ, Cowan IR, Farquhar GD (1997) The apparent feedforward response of stomata to air vapour pressure deficit: information revealed by different experimental procedures with two rainforest trees. Plant Cell Environ 20:142–145.

Franks PJ, Berry JA, Lombardozzi DL, Bonan GB (2017) Stomatal function across temporal and spatial scales: deep-time trends, land-atmosphere coupling and global models. Plant Physiol 174:583–602.

Gimeno TE, Crous KY, Cooke J, O'Grady AP, Ósvaldsson A, Medlyn BE, Ellsworth DS (2015) Conserved stomatal behaviour under elevated CO_2 and varying water availability in a mature woodland. Funct Ecol 30:700–709.

Gimeno TE, McVicar TR, O'Grady AP, Tissue DT, Ellsworth DS (2018) Elevated CO_2 did not affect the hydrological balance of a mature native eucalyptus woodland. Glob Chang Biol 33:0–2.

Gimeno TE, Saavedra N, Ogée J, Medlyn BE, Wingate L (2019) A novel optimization approach incorporating non-stomatal limitations predicts stomatal behaviour in species from six plant functional types. J Exp Bot 70:1639–1651.

Huang LF, Zheng JH, Zhang YY, Hu WH, Mao WH, Zhou YH, Yu JQ (2006) Diurnal variations in gas exchange, chlorophyll fluorescence quenching and light allocation in soybean leaves: the cause for midday depression in CO_2 assimilation. Sci Hortic (Amsterdam) 110:214–218.

Kala J, De Kauwe MG, Pitman AJ, Medlyn BE, Wang YP, Lorenz R, Perkins-Kirkpatrick SE (2016) Impact of the representation of stomatal conductance on model projections of heatwave intensity. Sci Rep 6:1–7.

Keenan T, Sabate S, Gracia C (2010) Soil water stress and coupled photosynthesis-conductance models: bridging the gap between conflicting reports on the relative roles of stomatal, mesophyll conductance and biochemical limitations to photosynthesis. Agric For Meteorol 150:443–453.

Knauer J, Werner C, Zaehle S (2015) Evaluating stomatal models and their atmospheric drought response in a land surface scheme: a multibiome analysis. J Geophys Res Biogeogr 120:1894–1911.

Knauer J, Zaehle S, De Kauwe MG, Bahar NHA, Evans JR, Medlyn BE, Reichstein M, Werner C (2019) Effects of mesophyll conductance on vegetation responses to elevated CO_2 concentrations in a land surface model. Glob Chang Biol 25:1820–1838.

Kowalczyk EA, Wang YP, Law RM (2006) The CSIRO atmosphere biosphere land exchange (CABLE) model for use in climate models and as an offline model. CSIRO Marine and Atmospheric Research Paper 013 .

Lawlor DW, Cornic G (2002) Photosynthetic carbon assimilation and associated metabolism in relation to water deficits in higher plants. Plant Cell Environ 25:275–294.

Lawlor DW, Tezara W (2009) Causes of decreased photosynthetic rate and metabolic capacity in water-deficient leaf cells: a critical evaluation of mechanisms and integration of processes. Ann Bot 103:561–579.

Leuning R (1995) A critical appraisal of a combined stomatal- photosynthesis model for C3 plants. Plant Cell Environ 18:339–355.

Li X, Blackman CJ, Choat B, Duursma RA, Rymer PD, Medlyn BE, Tissue DT (2018) Tree hydraulic traits are coordinated and strongly linked to climate-of-origin across a rainfall gradient. Plant Cell Environ 41:646–660.

MacFarlane C, White DA, Adams MA (2004) The apparent feed-forward response to vapour pressure deficit of stomata in droughted, field-grown *Eucalyptus globulus* Labill. Plant Cell Environ 27:1268–1280.

Medlyn BE, Duursma RA, Eamus D, et al. (2011) Reconciling the optimal and empirical approaches to modelling stomatal conductance. Glob Chang Biol 17:2134–2144.

Medlyn BE, Dreyer E, Ellsworth D, Forstreuter M, Harley PC, Kirschbaum MUF, Le Roux X, Montpied P, Strassemeyer J, Walcroft A, Wang K, Loustau D (2002) Temperature response of parameters of a biochemically based model of photosynthesis. II. A review of experimental data. Plant, Cell Environ 25:1167–1179.

Mediavilla S, Santiago H, Escudero A (2002) Stomatal and Mesophyll Limitations to Photosynthesis in One Evergreen and One Deciduous Mediterranean Oak Species. Photosynthetica 40:553–559.

Monteith JL (1995) A reinterpretation of stomatal responses to humidity. Plant Cell Environ 18:357–364.

Monteith JL, Unsworth MH (Fourth Edition) (2013) Principles of Environmental Physics. Academic Press, Oxford, UK.

Mott KA, Buckley TN (1998) Stomatal heterogeneity. J Exp Bot 49:407–417.

Nascimento HCS, Marenco RA, (2013) Mesophyll conductance variations in response to diurnal environmental factors in Myrcia paivae and Minquartia guianensis in Central Amazonia. Photosynthetica 51:457–464.

Neufeld HS, Grantz DA, Meinzer FC, Goldstein G, Crisosto GM, Crisosto C, (1992) Genotypic Variability in Vulnerability of Leaf Xylem to Cavitation in Water-Stressed and Well-Irrigated Sugarcane. Plant Physiol 100:1020–1028.

Niinemets Ü, Wright IJ, Evans JR (2009) Leaf mesophyll diffusion conductance in 35 Australian sclerophylls covering a broad range of foliage structural and physiological variation. J Exp Bot 60:2433–2449.

North GB, Nobel PS (1997) Root-soil contact for the desert succulent *Agave deserti* in wet and drying soil. New Phytol 135:21–29.

Novick KA, Ficklin DL, Stoy PC et al. (2016) The increasing importance of atmospheric demand for ecosystem water and carbon fluxes. Nat Clim Chang 1:1–5.

Ogle K, Barber JJ, Willson C, Thompson B (2009) Hierarchical statistical modeling of xylem vulnerability to cavitation: methods. New Phytol 182:541–554.

Oren R, Sperry JS, Katul GG, Pataki DE, Ewers BE, Phillips N, Schäfer KVR (1999) Survey and synthesis of intra- and interspecific variation in stomatal sensitivity to vapour pressure deficit. Plant Cell Environ 22:1515–1526.

Paul MJ, Foyer CH (2001) Sink regulation of photosynthesis. J Exp Bot 52:1383–1400.

Reichstein M, Bahn M, Ciais P et al. (2013) Climate extremes and the carbon cycle. Nature 500:287–295.

Renchon AA, Griebel A, Metzen D et al. (2018) Upside-down fluxes down under: CO2 net sink in winter and net source in summer in a temperate evergreen broadleaf forest. Biogeosciences 15:3703–3716.

Reynolds JF, Smith DMS, Lambin EF et al. (2007) Global desertification: building a science for dryland development. Science 316:847–851.

Scoffoni C, Albuquerque C, Brodersen CR, Townes SV, John GP, Bartlett MK, Buckley TN, McElrone AJ, Sack L (2017) Outside-xylem vulnerability, not xylem embolism, controls leaf hydraulic decline during dehydration. Plant Physiol 173:1197–1210.

Sperry JS, Donnelly JR, Tyree MT (1988) A method for measuring hydraulic conductivity and embolism in xylem. Plant Cell Environ 11:35–40.

Sperry JS, Hacke UG, Oren R, Comstock JP (2002) Water deficits and hydraulic limits to leaf water supply. Plant Cell Environ 25:251–263.

Tezara W, Mitchell VJ, Driscoll SD, Lawlor DW (1999) Water stress inhibits plant photosynthesis by decreasing coupling factor and ATP. Nature 401:914–917.

Thomas DS, Eamus D (1999) The influence of predawn leaf water potential on stomatal responses to atmospheric water content at constant *C*(i) and on stem hydraulic conductance and foliar ABA concentrations. J Exp Bot 50:243–251.

Tuzet A, Perrier A, Leuning R (2003) A coupled model of stomatal conductance, photosynthesis and transpiration. Plant Cell Environ 26:1097–1116.

Tyree MT, Sperry JS (1989) Vulnerability of Xylem to Cavitation and Embolism. Annu Rev Plant Physiol Plant Mol Biol 40:19–36.

Verhoef A, Egea G (2014) Modeling plant transpiration under limited soil water: comparison of different plant and soil hydraulic parameterizations and preliminary implications for their use in land surface models. Agric For Meteorol 191:22–32.

Warren CR (2008) Soil water deficits decrease the internal conductance to CO2 transfer but atmospheric water deficits do not. J Exp Bot 59:327–334.

Whitley R, Taylor D, Macinnis-Ng C, Zeppel M, Yunusa I, O'Grady A, Froend R, Medlyn B, Eamus D (2013) Developing an empirical model of canopy water flux describing the common response of transpiration to solar radiation and VPD across five contrasting woodlands and forests. Hydrol Process 27:1133–1146.

Will RE, Wilson SM, Zou CB, Hennessey TC (2013) Increased vapor pressure deficit due to higher temperature leads to greater transpiration and faster mortality during drought for tree seedlings common to the forest-grassland ecotone. New Phytol 200:366–374.

Woodward FI, Smith TM, Emanuel WR (1995) A global land primary productivity and phytogeography model. Global Biogeochem Cycles 9:471–490.

Wujeska-Klause A, Crous KY, Ghannoum O, Ellsworth DS (2019) Lower photorespiration in elevated CO 2 reduces leaf N concentrations in mature *Eucalyptus* trees in the field. Glob Chang Biol 25:1282–1295.

Yang S, Tyree MT (1994) Hydraulic architecture of *Acer saccharum* and *A. rubrum*: comparison of branches to whole trees and the contribution of leaves to hydraulic resistance. J Exp Bot 45:179–186.

Zeppel M, MacInnis-Ng C, Palmer A, Taylor D, Whitley R, Fuentes S, Yunusa I, Williams M, Eamus D (2008) An analysis of the sensitivity of sap flux to soil and plant variables assessed for an Australian woodland using a soil-plant-atmosphere model. Funct Plant Biol 35:509–520.

Zhou S, Duursma R A, Medlyn BE, Kelly JWG, Prentice IC (2013) How should we model plant responses to drought? An analysis of stomatal and non-stomatal responses to water stress. Agric For Meteorol 182–183:204–214.

Zhou S, Medlyn B, Sabate S, Sperlich D, Prentice IC (2014) Short-term water stress impacts on stomatal, mesophyll and biochemical limitations to photosynthesis differ consistently among tree species from contrasting climates. Tree Physiol 34:1035–1046.